Title	Ab initio calculation of transverse spin current in graphene nanostructures
Author(s)	Wang, B; Wang, J; Guo, H
Citation	Physical Review B: Condensed Matter and Materials Physics, 2009, v. 79 n. 16 article no. 165417
Issued Date	2009
URL	http://hdl.handle.net/10722/80754
Rights	Creative Commons: Attribution 3.0 Hong Kong License

Ab initio calculation of transverse spin current in graphene nanostructures

Bin Wang,[1] Jian Wang,[1,*] and Hong Guo[2]
[1]*Department of Physics, The University of Hong Kong, Pokfulam Road, Hong Kong, China*
[2]*Department of Physics and Center for the Physics of Materials, McGill University, Montreal, Quebec, Canada H3A 2T8*
(Received 22 February 2009; published 13 April 2009)

We report a theoretical analysis of transverse spin current in a four-probe graphene nanostructure in the absence of spin-orbit interaction and magnetic field. The nanostructure consists of a finite-size graphene sheet connected to the outside world by two zigzag graphene nanoribbons (GNR) and two armchair graphene nanoribbons, forming a cross-shaped two-dimensional device. Due to edge state induced magnetism at zigzag GNR boundaries, our result shows that a pure transverse spin current without an accompanying charge current is induced. We have calculated the transverse spin conductance by an atomic first-principles method where density-functional theory is carried out within the Keldysh nonequilibrium Green's function framework.

DOI: 10.1103/PhysRevB.79.165417 PACS number(s): 85.35.−p, 71.15.Mb, 73.63.−b, 81.05.Uw

I. INTRODUCTION

Several years ago Murakami *et al.*[1] proposed a notion of dissipationless spin current that has generated considerable interest in the literature. For device samples having a finite extent, the flow of spin current can cause spin accumulation at edges of the sample, resulting to a situation that spin-up electrons accumulate at one edge while spin-down electrons at the opposite edge.[2] Hence a spin-Hall effect (SHE) (Refs. 3 and 4) is produced where chemical potentials for the two spin channels become different at the two edges of the sample. In semiconductor samples, intrinsic SHE is shown to occur due to spin-orbital (SO) interactions.[1,4]

In a very interesting paper, Kane and Mele[5] proposed that an intrinsic *quantized* SHE is possible in two-dimensional graphene due to SO interaction coupled to the peculiarity of graphene electronic structure. However, it was pointed out by a number of authors[6] that SO interaction in graphene is extremely weak, ~0.01 meV, so that the intrinsic SHE cannot be easily observed in realistic experimental conditions. Nevertheless, large noninteger spin-Hall conductance can become measurable experimentally in the metallic regime.[7] In addition, it appears that integer SHE can be induced *extrinsically* in graphene driven by an external magnetic field.[8]

In this work, we show that it is actually possible to generate a transverse spin current electrically in graphene nanostructures without SO interaction and without external magnetic field. The intrinsic physics behind this is due to electronic structure of zigzag graphene nanoribbon (GNR). It has been known that zigzag GNR has magnetic edge states along the zigzag ribbon boundaries,[9–11] namely, the atoms are spin polarized along the zigzag edge due to localized electronic structure at those locations. On the other hand, an armchair GNR does not have magnetic edge. We find that a four-probe graphene cross formed by two zigzag GNRs and two armchair GNRs can produce transverse spin current.[12] The mechanism we have discovered is purely electronic, i.e., intrinsic to the graphene nanostructure. We have carried out extensive first-principles calculations to investigate this effect.

Theoretical study of edge magnetism in graphene nanoribbon[9,10] dates back to before the recent seminal papers of experimental work on single sheet graphene.[13] In particular, when a zigzag GNR is monohydrogenated at one edge and dihydrogenated at the other edge, it was found that a net and finite magnetic moment **M** appears in the zigzag GNR (Ref. 10) due to localized electronic states going along the zigzag GNR edges at zero temperature. If both edges are monohydrogenated, edge magnetism still occurs but the moments on the two edges tend to point to opposite direction with a tiny energy loss over the ferromagnetic configuration when all moments point to the same direction. In other words, ferromagnetic coupling crossing the ribbon width is slightly more favored than antiferromagnetic. The edge magnetism has recently been subjected to extensive theoretical investigations and, importantly, it appears to survive weak disorder at the zigzag GNR edge.[11] To save space, we refer interested readers to the original literature on the physics of edge magnetism in zigzag GNR.[9–11] In the following, by first-principles calculation, we show that this edge magnetism gives rise to a pure transverse spin current in graphene nanostructures.

II. THEORY AND NUMERICAL RESULTS

The four-probe graphene nanostructure we consider is shown in Fig. 1. The device consists of a central scattering region (indicated by the square box) connected by four semi-infinite GNR as device leads. In particular, we use two armchair GNR leads along the x direction and two zigzag GNR leads along the z direction. The carbon atoms at edges of the two armchair GNRs are saturated by hydrogen atoms. The zigzag GNRs are monohydrogenated on the upper edge and dihydrogenated on the lower edge.[10] The system is symmetric about x axis. Therefore, for this device edge magnetism exists on the left and right leads (zigzag GNR), and there is no magnetism on the top and bottom leads (armchair GNR). Note that the experimental fabrication of GNR that is as narrow as 2 nm has been realized.[14] We imagine that the four-probe graphene nanostructure may possibly be made by fusing two narrow GNRs, or by cutting four corners of a square graphene sheet using oxygen plasma technique.[15] Because the two zigzag GNR electrodes have edge magnetism, there are two possible configurations of the moments. First,

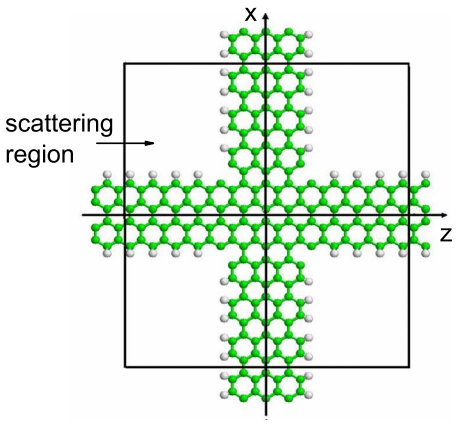

FIG. 1. (Color online) Atomic geometry of the four-probe graphene nanostructure. The left/right (L,R) leads are zigzag GNRs, monohydrogenated on the upper edge, and dihydrogenated on the lower edge of the region. The up/down (U,D) leads are armchair GNRs monohydrogenated on both edges.

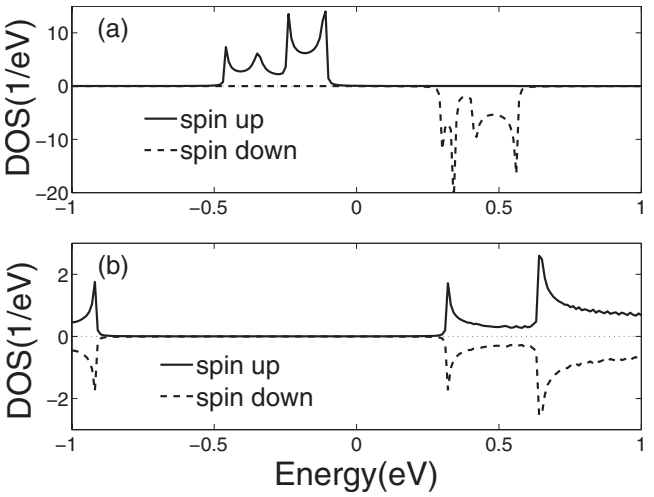

FIG. 2. (a) Spin resolved DOS of a zigzag GNR. (b) DOS of an armchair GNR. The positions of E_F are set to zero as indicated by the horizontal line.

magnetic moments $\mathbf{M}_{L/R}$ of the left and right leads (zigzag GNRs) are parallel, i.e., $\mathbf{M}_L=\mathbf{M}_R$. Second, they are antiparallel, $\mathbf{M}_L=-\mathbf{M}_R$. It turns out that antiparallel configuration induces an anomalous spin-Hall effect, namely, a pure spin current can flow between armchair GNR leads when zigzag GNR leads are biased by an external voltage (see below).

The atomic structure of the scattering region (see Fig. 1) for both parallel and antiparallel configurations is relaxed using the total-energy density-functional theory (DFT) package SIESTA.[16] During the relaxation, each lead included in the scattering region must be long enough to ensure that the potential at the boundary be the same as that of the semi-infinite lead.[17] Calculation shows that the geometry optimization does not considerably change the atomic structure from the ideal one. The total energy of the four-probe device with parallel configuration is slightly lower than that of antiparallel configuration. Obviously, this energy difference is only associated with the formation of domain wall in the center of the device and diminishes as the size of device increases. Hence it can be easily overcome in realistic experimental situations. Once the scattering region is relaxed, the four leads are extended to infinity to form the four-probe transport junctions of Fig. 1 for quantum transport calculations at finite bias. For nonequilibrium transport calculation, we use the state-of-the-art first-principles quantum transport package MATDCAL (Refs. 18 and 19), where DFT is carried out within the Keldysh nonequilibrium Green's function formalism (NEGF).[20] Within NEGF-DFT the device Hamiltonian and electronic structure are determined by DFT, the nonequilibrium quantum statistics of the device physics is determined by NEGF, and the transport boundary conditions under external bias are handled by real-space numerical techniques.

Details of the two-probe NEGF-DFT implementation can be found in Refs. 18 and 19, and further calculation details of this work are given in Ref. 20. The extension to four probes is to include into the retarded Green's function,

$$G^r = \frac{1}{E - H - \Sigma^r}, \tag{1}$$

a four-probe self-energy

$$\Sigma^r = \Sigma_L^r + \Sigma_R^r + \Sigma_D^r + \Sigma_U^r, \tag{2}$$

which describes coupling of the scattering region to the four semi-infinite leads labeled by L, R, D, and U (the left, right, down, and up leads).[21,22] Σ^r is obtained by standard iterative method for the periodic lattice of graphene ribbons.[19] The transmission coefficient for spin channel σ is obtained from NEGF as[21,23]

$$T_{ij\sigma}(E) = \mathrm{Tr}[\Gamma_i G^r \Gamma_j G^a]_{\sigma\sigma}, \tag{3}$$

where indices i,j are any of L, R, D, and U, T_{ij} indicates transmission coefficient from j lead to i lead, σ labels spin configuration, and $\Gamma_i = i(\Sigma_i^r - \Sigma_i^a)$. We consider collinear moments and neglect spin-orbit interaction.[6]

The density of states (DOS) of the zigzag GNR is shown in Fig. 2(a) where a gap separating spin-up and spin-down channels appears near the Fermi level as expected.[9–11] In comparison, Fig. 2(b) shows DOS of an armchair GNR. Comparing DOS of zigzag GNR and armchair GNR, we observe that there is little overlap for spin-up channels between the left zigzag GNR lead and the down armchair GNR lead in the energy range of $-1-1$ eV, indicating a half-metallic behavior[11] in this range of energy. Hence, spin-up electrons cannot traverse between left and down leads. For spin-down channel, DOS of the left zigzag GNR lead overlaps with that of the down armchair GNR lead for energy range 0.25 eV $< E <$ 0.6 eV. As a result, transmission of electrons is allowed only for spin-down channel in the energy window [0.25 eV, 0.6 eV].

The transverse spin conductance can be calculated as follows. We apply a very small external bias V_i to the four leads $i=(L,U,R,D)$ as $V_i=(v/2,0,-v/2,0)$, i.e., biasing the L and R leads, and measure charge and the transverse spin conductance G_{ch} and G_{sp} between $i=D,U$, i.e., transverse to the

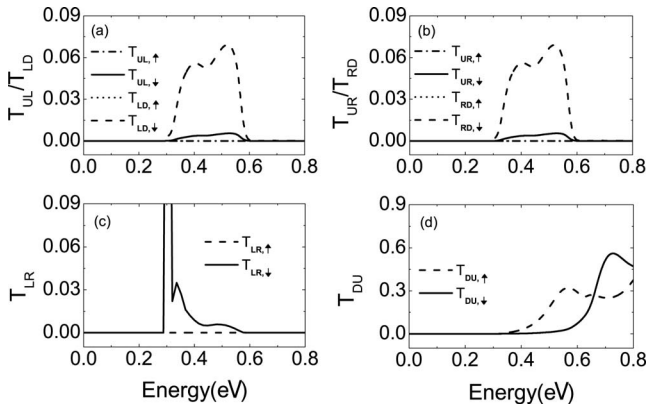

FIG. 3. Spin dependent transmission coefficients for parallel configuration. (a) From left (up) to up (left) leads and from down (left) to left (down) leads. (b) From right (up) to up (right) leads and from down (right) to right (down) leads. (c) From right (left) to left (right). (d) From up (down) to down (up).

external electric field. Since $T_{\alpha\beta\sigma}$ is the transmission coefficient from lead β to lead α with spin index $\sigma=\uparrow\downarrow$ or $\pm$, the charge current from lead β to α is given by $(e^2/h)T_{\alpha\beta\sigma}(v_\beta - v_\alpha)$. Similarly, the spin current from lead β to α is given by $\sigma(e/4\pi)T_{\alpha\beta\sigma}(v_\beta - v_\alpha)$. According to the multiprobe Landauer-Büttiker formula, the charge and spin currents through lead α is given by

$$I_\alpha = (e^2/h)\sum_{\beta\sigma} T_{\alpha\beta\sigma}(v_\beta - v_\alpha),$$

$$I_{s\alpha} = (e/4\pi)\sum_{\beta\sigma} \sigma T_{\alpha\beta\sigma}(v_\beta - v_\alpha). \quad (4)$$

For our setup, the transverse charge conductance $G_{\rm ch}$ and transverse spin conductance $G_{\rm sp}$ can be calculated from[24–26]

$$G_{\rm ch} = (e^2/2h)[(T_{DL\uparrow} + T_{DL\downarrow}) - (T_{DR\uparrow} + T_{DR\downarrow})],$$

$$G_{\rm sp} = (e/8\pi)[(T_{DL\uparrow} - T_{DL\downarrow}) - (T_{DR\uparrow} - T_{DR\downarrow})]. \quad (5)$$

Hence, the behavior of transmission T_{ij} determines these transport quantities.

Figure 3 plots transmission coefficient of parallel configuration. The following observations are in order. (1) Since the left/right leads only allow electron to transmit in spin-down channel in the energy range [0.25 eV, 0.6 eV], only spin-down components of T_{UL}, T_{UR}, T_{LD}, T_{RD}, and T_{LR} are nonzero. For T_{DU}, electron can transmit in both spin-up and spin-down channels. Since zigzag GNR leads are ferromagnetic, the scattering potential in the central region is spin dependent due to proximity effect or due to evanescent modes in the language of scattering theory. Therefore, when a charge is injected from the down lead, its spin must be influenced by the spin-polarized potential and it exits from the upper lead with a spin dependent transmission coefficient. Therefore T_{DU} is spin polarized and this polarization persists for energy larger than 0.6 eV. (2) Because the device is symmetric about x axis, we have $T_{UL,\downarrow}=T_{UR,\downarrow}$ and $T_{LD,\downarrow}=T_{RD,\downarrow}$. (3) Comparing the curves in Fig. 3(a), $T_{LD,\downarrow}$ is of one order of magnitude larger than $T_{UL,\downarrow}$. This means that the spin-down electrons are more likely to transfer to the D lead than to the U lead when a small bias is applied between L and R leads given the fact that T_{LD} equals to T_{DL}. This is understandable because the L (or R) lead is not symmetric about the z axis due to different numbers of H atoms on up and down edges of the zigzag GNR. More quantitatively, Fig. 4 plots the real-space projection on the x-z plane of the spin-down electron density in parallel configuration, obtained by integrating density along the y axis. Figure 4 shows that the spin-down density in the down edge is larger than that in the upper edge for left/right zigzag GNR leads, indicating that more electrons are traversing to the D lead. (4) Since all the spin-up channels of transmission coefficients appearing in Eq. (5) are closed, both $G_{\rm ch}$ and $G_{\rm sp}$ are zero (see Fig. 3). We conclude that no spin-Hall effect is possible in parallel configuration.

For antiparallel configuration, we expect only spin-down channel in the left zigzag GNR lead and only spin-up channel in the right zigzag GNR lead for transport. This is confirmed in Fig. 5 where the calculated $T_{UL,\uparrow}=T_{LD,\uparrow}=T_{UR,\downarrow}=T_{RD,\downarrow}=0$. Different from parallel configuration, we found $T_{LR,\uparrow}=T_{LR,\downarrow}=0$ since there is no overlap between DOS of the left and right leads in the relevant energy range. Because spin-down electron distribution of the L lead is equal to the spin-up electron distribution of the R lead, we have $T_{UL,\downarrow}=T_{UR,\uparrow}$ and $T_{LD,\downarrow}=T_{RD,\uparrow}$. In addition, because the density of spin-down electron on the lower edge of the left zigzag GNR lead is much larger than that on the upper edge, we have $T_{LD,\downarrow} \gg T_{UL,\downarrow}$. For the R lead, it is the spin-up electron density that is larger at the lower edge, resulting $T_{RD,\uparrow} \gg T_{UR,\uparrow}$. Furthermore, Fig. 5(d) shows that $T_{DU,\uparrow}=T_{DU,\downarrow}$: this is because spin-down channel of the left zigzag GNR lead plays the same role as spin-up channel of the right zigzag GNR lead; thus the influence of left lead to spin-down transport between leads U and D must be the same as the influence of the right lead to spin up. Using $T_{DL\uparrow}=T_{DR\downarrow}=0$ and $T_{DL\downarrow}=T_{DR\uparrow}$, from Eq. (5) we obtain

$$G_{\rm ch}=0, \quad G_{\rm sp}=-\left(\frac{e}{4\pi}\right)T_{DL\downarrow}, \quad (6)$$

where $T_{DL\downarrow}=T_{LD\downarrow}$ is shown in Fig. 5(a). Hence a pure spin current, without an accompanying charge current, is induced in antiparallel configuration devices.

In order to observe the transverse spin current experimentally, one probably needs a wider GNR than what we have calculated here. To address this issue, we have done *ab initio* calculations of the magnetic moment of several wider straight zigzag GNRs (a straight GNR is much easier to calculate than the four-probe device) using DFT and found that they indeed possess finite magnetic moment. In particular the band structures of zigzag GNR were calculated for ribbons with width $d=1.27$, 1.7, 2.6, and 4.8 nm. These widths are within reach by the fabrication technique in Ref. 14. We have the following observations. First, there is always a gap between the spin-up and spin-down channels near the Fermi level for all ribbon widths. Therefore, in the energy range [0, 0.8] eV, only spin-down (up) electrons can be injected into the device from left (right) lead for antiparallel configuration of the moments in the four-probe device. This agrees

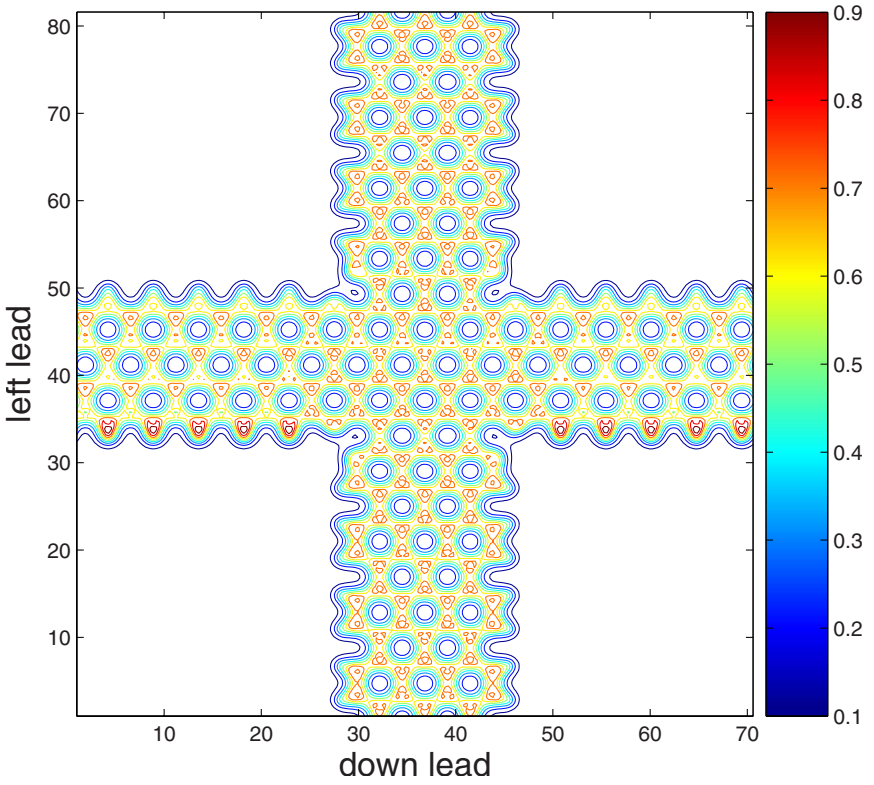

FIG. 4. (Color online) Real-space projection of spin-down electron density on the *x*-*z* plane for parallel configuration. Note the clear difference between densities at the lower edge and the upper edge of the left/right zigzag GNR leads.

with the result discussed above. Second, the complete spin-polarized flatband near the Fermi level gives rise to a finite magnetic moment on the edge (see detailed discussion in Ref. 10), which led to the transverse spin current in our four-probe device structure. Since the presence of ferromagnetic leads is the key of this effect, as long as finite magnetic moments exists for wider zigzag GNRs, the transverse spin current should remain.

Furthermore, our calculation for wider GNR shows that a magnetic moment exists on each edge carbon atom. Importantly, finite magnetic moments also appear on two hydrogen atoms at the bihydrogenated edge. For GNRs with width d =1.27, 1.7, 2.6, and 4.8 nm, the total magnetic moments on the dihydrogenated edges (including one C atom and two hydrogen atoms) are 0.0663, 0.0637, 0.1065, and 0.1060 Bohr magneton, respectively. The magnetic moment of these hydrogen atoms is along the same direction as that of carbon atom on the other edge, resulting to a ferromagnetic state.

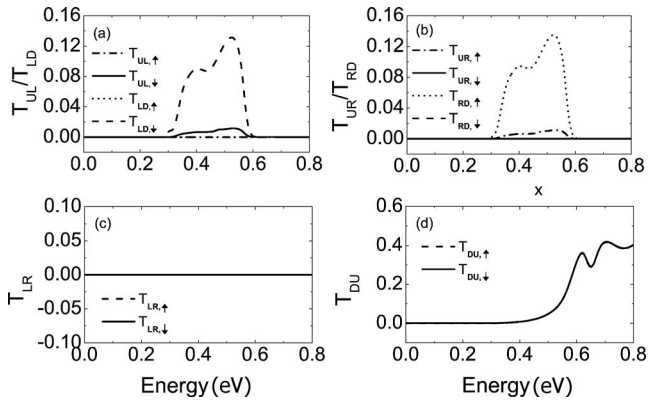

FIG. 5. Spin dependent transmission of antiparallel configuration at zero bias. (a) From left (up) to up (left) lead and from down (left) to left (down) lead. (b) From right (up) to up (right) lead and from down (right) to right (down) lead. (c) From right (left) to left (right) lead. (d) From up (down) to down (up) lead.

Theoretically, the formation of a ferromagnetic state in our GNR has a very strong reason. For the zigzag ribbon, there are $2N$ carbon atoms in a unit cell where N is the number of bipartite lattice sites. Due to the formation of $sp3$ bonds at the bihydrogenated edge, only $2N$-1 carbon atoms have electrons in a unit cell resulting to an imbalance of number of electrons in the sublattices. According to Lieb's theorem,[27] the ground state of such a configuration must be a ferromagnetic state with finite magnetization. Our *ab initio* result is totally consistent with Lieb's theorem.

III. SUMMARY

In summary, by *ab initio* NEGF-DFT calculations we have shown that a pure transverse spin current can be generated without spin-orbital interaction and without external magnetic field. This effect is due to edge magnetism that occurs in the zigzag GNR—an intrinsic property of graphene nanoribbons. The value of the transverse spin conductance G_{sp} of the graphene nanostructure is rather large, being similar in magnitude as that of 2D mesoscopic semiconductor devices in which the SHE is generated by large Rashba spin-orbital interactions.[25,26] Since 1D magnetic order due to short-range interactions does not survive thermal fluctuation in the *thermodynamic limit*, we expect the transverse spin current discussed here to exist in nanoscale samples.

ACKNOWLEDGMENTS

We gratefully acknowledge V. Timochevski for his help in

calculations of zigzag GNR edge magnetism. This work was financially supported by RGC Grant (Grant No. HKU 7048/06P) from the government SAR of Hong Kong and LuXin Energy Group. H.G. is supported by NSERC of Canada, FQRNT of Québec and Canadian Institute of Advanced Research.

*jianwang@hkusub.hku.hk

[1] S. Murakami, N. Nagaosa, and S. C. Zhang, Science **301**, 1348 (2003).
[2] Y. K. Kato, R. C. Myers, A. C. Gossard, and D. D. Awschalom, Science **306**, 1910 (2004).
[3] J. E. Hirsch, Phys. Rev. Lett. **83**, 1834 (1999).
[4] J. Sinova, D. Culcer, Q. Niu, N. A. Sinitsyn, T. Jungwirth, and A. H. MacDonald, Phys. Rev. Lett. **92**, 126603 (2004).
[5] C. L. Kane and E. J. Mele, Phys. Rev. Lett. **95**, 226801 (2005).
[6] H. Min, J. E. Hill, N. A. Sinitsyn, B. R. Sahu, L. Kleinman, and A. H. MacDonald, Phys. Rev. B **74**, 165310 (2006).
[7] N. A. Sinitsyn, J. E. Hill, H. Min, J. Sinova, and A. H. MacDonald, Phys. Rev. Lett. **97**, 106804 (2006).
[8] D. A. Abanin, P. A. Lee, and L. S. Levitov, Phys. Rev. Lett. **96**, 176803 (2006).
[9] K. Nakada, M. Fujita, G. Dresselhaus, and M. S. Dresselhaus, Phys. Rev. B **54**, 17954 (1996). In this work, there is no hydrogenation at the edge of GNR.
[10] K. Kusakabe and M. Maruyama, Phys. Rev. B **67**, 092406 (2003).
[11] Y. W. Son, M. L. Cohen, and S. G. Louie, Nature (London) **444**, 347 (2006).
[12] We note that the spin injection and spin accumulation of four terminal hybrid mesoscopic devices has been studied extensively. See N. Tombros, S. J. van der Molen, and B. J. van Wees, Nature **448**, 571 (2007); Phys. Rev. B **73**, 233403 (2006).
[13] K. S. Novoselov, A. K. Geim, S. V. Morozov, D. Jiang, Y. Zhang, S. V. Dubonos, I. V. Grigorieva, and A. A. Firsov, Science **306**, 666 (2004); K. S. Novoselov, A. K. Geim, S. V. Morozov, D. Jiang, M. I. Katsnelson, I. V. Grigorieva, S. V. Dubonos, and A. A. Firsov, Nature (London) **438**, 197 (2005); Y. Zhang, Y. Tan, H. L. Stormer, and P. Kim, *ibid.* **438**, 201 (2005); K. S. Novoselov, E. McCann, S. V. Morozov, V. I. Fal'ko, M. I. Katsnelson, U. Zeitler, D. Jiang, F. Schedin, and A. K. Geim, Nat. Phys. **2**, 177 (2006).
[14] X. Wang, Y. Ouyang, X. Li, H. Wang, J. Guo, and H. Dai, Phys. Rev. Lett. **100**, 206803 (2008).
[15] X. Guo, J. P. Small, J. E. Klare, Y. Wang, M. S. Purewal, I. W. Tam, B. H. Hong, R. Caldwell, L. Huang, S. O'Brien, J. Yan, R. Breslow, S. J. Wind, J. Hone, P. Kim, and C. Nuckolls, Science **311**, 356 (2006).
[16] P. Ordejón, E. Artacho, and J. M. Soler, Phys. Rev. B **53**, R10441 (1996); J. M. Soler, E. Artacho, J. D. Gale, A. García, J. Junquera, P. Ordejón, and D. Sánchez-Portal, J. Phys.: Condens. Matter **14**, 2745 (2002).
[17] For SIESTA structural relaxation, we use 20×20 k mesh for sampling the two-dimensional first Brillouin zone (k_x,k_z). A conjugate gradient method is used to achieve total-energy minimization with a restriction of planar configuration until the residual force on each atom is less than 0.05 eV/Å. The relaxed bond length of the nearest C-C bond, C-H bond at monohydrogenated sites of ZGNR, C-H bond at dihydrogenated sites of zigzag GNR (ZGNR), and C-H bond at monohydrogenated sites of armchair GNR (AGNR), are found to be 41.40, 1.115, 1.136, and 0.977 Å, respectively.
[18] D. Waldron, P. Haney, B. Larade, A. MacDonald, and H. Guo, Phys. Rev. Lett. **96**, 166804 (2006); D. Waldron, V. Timoshevskii, Y. Hu, K. Xia, and H. Guo, *ibid.* **97**, 226802 (2006).
[19] J. Taylor, H. Guo, and J. Wang, Phys. Rev. B **63**, 245407 (2001); **63**, 121104 (2001).
[20] For NEGF-DFT transport analysis, a single-zeta s,p,d linear combination of atomic orbital basis set is used; atomic cores are defined by standard nonlocal norm conserving pseudopotential [N. Troullier and J. L. Martins, Phys. Rev. B **43**, 1993 (1991)] The exchange correlation is treated at the local spin density approximation (LSDA) level [U. von Barth and L. Hedin, J. Phys. C **5**, 1629 (1972)]. The NEGF-DFT self-consistency is controlled by a numerical tolerance of 10^{-4} eV.
[21] B. G. Wang, J. Wang, and H. Guo, J. Phys. Soc. Jpn. **70**, 2645 (2001).
[22] H. Mehrez, J. Taylor, H. Guo, J. Wang, and C. Roland, Phys. Rev. Lett. **84**, 2682 (2000).
[23] We have neglected spin-relaxation mechanisms due to the long spin-relaxation length in graphene (see Tombros *et al.* in Ref. 12).
[24] E. M. Hankiewicz, L. W. Molenkamp, T. Jungwirth, and J. Sinova, Phys. Rev. B **70**, 241301(R) (2004).
[25] L. Sheng, D. N. Sheng, and C. S. Ting, Phys. Rev. Lett. **94**, 016602 (2005).
[26] W. Ren, Z. H. Qiao, J. Wang, Q. F. Sun, and H. Guo, Phys. Rev. Lett. **97**, 066603 (2006).
[27] E. H. Lieb, Phys. Rev. Lett. **62**, 1201 (1989).